metals

MDPI

Article

Structure and Thermal Properties of an Al-Based Metallic Glass-Polymer Composite

Vladislav Zadorozhnyy [1,2,*], Margarita Churyukanova [1], Andrey Stepashkin [1], Mikhail Zadorozhnyy [1], Adit Sharma [1], Dmitry Moskovskikh [1], Junqiang Wang [3], Elena Shabanova [1], Sergey Ketov [2], Dmitry Louzguine-Luzgin [4,5] and Sergey Kaloshkin [1]

1 National University of Science and Technology MISIS, Leninsky prosp., 4, Moscow 119049, Russia; mch@misis.ru (M.C.); a.stepashkin@misis.ru (A.S.); zadorozhnyy.mihail@gmail.com (M.Z.); adit15@yandex.com (A.S.); mos@misis.ru (D.M.); ibloko1504@gmail.com (E.S.); kaloshkin@misis.ru (S.K.)
2 Erich Schmid Institute of Materials Science, Austrian Academy of Sciences, 8700 Leoben, Austria; ketov.sergey@gmail.com
3 Key Laboratory of Magnetic Materials and Devices, and Zhejiang Province Key Laboratory of Magnetic Materials and Application Technology, Ningbo Institute of Materials Technology and Engineering, Chinese Academy of Sciences, Ningbo 315201, China; jqwang@nimte.ac.cn
4 WPI Advanced Institute for Materials Research, Tohoku University, Sendai 980-8577, Japan; dml@wpi-aimr.tohoku.ac.jp
5 Mathematics for Advanced Materials-OIL, National Institute of Advanced Industrial Science and Technology (AIST), Sendai 980-8577, Japan
* Correspondence: zadorozhnyyvlad@gmail.com; Tel.: +7-495-638-44-13

Received: 30 October 2018; Accepted: 4 December 2018; Published: 7 December 2018

Abstract: A composite material based on polyethylene terephthalate (PET, about 1% by mass) and $Al_{85}Y_8Ni_5Co_2$ metallic glass was obtained by mechanical alloying and consequent spark plasma sintering. The spark plasma sintering was performed at a temperature near to the super cooled liquid region of the metallic glass. Mechanical properties and the structural characterization of the composite material were obtained. It was conceived that composite samples ($Al_{85}Y_8Ni_5Co_2$/PET) have a better thermal conductivity in comparison with pure PET samples. The formation of the crystalline phases causes degradation of physical properties. It was calculated that the activation energy for crystallization of the $Al_{85}Ni_5Y_8Co_2$ metallic glass is higher than that of the other types of metallic glasses ($Mg_{67.5}Ca_5Zn_{27.5}$ and $Cu_{54}Pd_{28}P_{18}$) used for composite preparation previously. This denotes a good thermal stability of the chosen metallic glass.

Keywords: composites; metallic glass; thermal properties; spark plasma sintering

1. Introduction

The unique properties of composite materials often make them more desirable than pure components. A combination of two different materials can result in enhanced properties, such as high strength and good ductility. The reinforcement elements help to improve the mechanical properties [1] of the composites. Metallic glasses have gained attention because of their remarkable properties [2]. They have outstanding corrosion and wear resistance and show unusual magnetic softness [3,4]. The procedure for casting metallic glasses is generally an inexpensive process. Metallic glasses have various applications in optical, electrical, magnetic, and mechanical materials, as well as in membranes, biological materials, and biotechnology [5].

Research activities have shown that polyethylene terephthalate (PET) can be used as an anti-friction polymer material [6]. The addition of a small quantity of polymer (PET) does not decrease the mechanical properties of the matrix that much during the process. The work of

Yusof et al. [7] confirmed that PET can be used as anti-friction material within aluminum alloys. A composite material with enhanced properties was obtained by Kundig et al. [8]. The process for composite material preparation is done by co-extrusion or ball milling [9–11]. PET can control electrical properties of the materials [12]. A functional block copolymer [13] structure can also be produced with metallic nanoparticles.

Metallic glasses, which have low glass transition temperatures near the melting point of the polymer, can be used to produce metallic glass polymer composites. This allows the con-thermal-plastic deformation. Al-based metal glasses are good choices for this purpose. For example, Wang et al. presented Al-based matrix composites, reinforced with different fillers, with good mechanical properties [14–18]. The twist extrusion technique was used for processing polymers with metallic glass, and the mechanical properties of aluminum based alloys were improved [19]. Therefore, this technique can be used for aluminum based alloys, especially for merging aluminum based metallic glasses. Various types of hybrid composite materials were also produced [19,20].

This work is an extension of the earlier works related to composite materials preparation. In the previous work [21], a composite material based on high-density polyethylene (HDPE) reinforced with $Mg_{67.5}Ca_5Zn_{27.5}$ metallic glass (about 10% by mass) was obtained by co-extrusion and compression. The co-extrusion and compression procedures were performed at the temperatures in the supercooled liquid temperature region for both materials, between the glass transition temperature (T_g) and crystallization temperature (T_x). It was found that the composite samples (HDPE/$Mg_{67.5}Ca_5Zn_{27.5}$) had excellent adhesion towards each other, good thermal conductivity, and high elastic modulus. In another study [22], bulk composites based on $Cu_{54}Pd_{28}P_{18}$ metallic glass and polytetrafluoroethylene (PTFE, about 1% by mass) were obtained by ball milling and subsequent spark plasma sintering (SPS) methods. The spark plasma sintering procedure was carried out at the temperature close to the supercooled liquid temperature region of the metallic glass. The mechanical and structural characterization of the obtained metallic glass/polymeric composite samples was performed. It was found that composite samples ($Cu_{54}Pd_{28}P_{18}$/PTFE) have better thermal conductivity in comparison with the pure PTFE samples. It was also shown that precipitation of the crystalline phases on the interface between the metallic glass particles leads to the degradation of their physical properties.

In the present work, the composite material based on the $Al_{85}Y_8Ni_5Co_2$ metallic glass mixed with polyethylene terephthalate (PET, about 1% BY mass) was obtained and studied. Investigations of the structure and thermal properties of the obtained composites were performed.

2. Materials and Methods

A metallic glass ribbon ($Al_{85}Y_8Ni_5Co_2$) was used for the sample preparation. Al-Y-Ni-Co alloy ingots were prepared by argon arc melting from the mixtures of pure Al, Ni, Co, and Y metals (purity of about 99.9% by mass). The ribbon samples were prepared by a copper roller melt spinning technique. The thickness of the resulting ribbon ranged from 0.02 to 0.03 mm, and the width ranged from 4.7 to 4.9 mm. A high density polyethylene terephthalate (PET) with an average particle size of about 200 μm was also used.

X-ray diffraction (XRD) experiments were performed with a DRON (CoKα radiation) diffractometer (Research and production enterprise "Bourevestnik", Saint Petersburg, Russian Federation) (2θ angles: from 10 to 120 degree. Step: 0.1 degree. Exposition time per step: 5 s. Beam size: 6–8 mm). The lattice parameters and phase compositions were determined with an accuracy of ±0.0001 nm and ±5%, respectively. The size of the crystallites in the powders was determined by the broadening of the diffraction pattern profiles with Cauchy functions. The accuracy of the crystallite size determination was ±1 nm. The percentage of the amorphous phase was determined, according to a kinematic standard method and annealed nickel powder as a standard [23].

The thermal properties of the prepared samples were examined using the NETZSCH DSC 204 F1 Phoenix Differential Scanning Calorimeter (DSC) (Netzsch Erich Netzsch GmbH & Co, Selb, Upper Franconia, Bavaria, Germany) with a heating rate of 10 °C/min. The maximum temperature was

600 °C for DSC and 350 °C for heat capacity measurement. The mass of the samples was 10–15 mg. The glass transition temperature (T_g) and the crystallization temperature (T_x) were estimated from the DSC curves using the standard computer application.

The Netzsch LFA 447 NanoFlash provided the thermal diffusivity analyses of composite materials. Composite materials have been studied in the temperature range from 25 to 200 °C. The thermal conductivity was analyzed, according to the requirements of ASTM E1461.

The density of the samples obtained was measured by the hydrostatic weighing method using an analytical balance and the GR-202, using the density determination set and AD-1653, in ethanol.

Thermal conductivity of the samples was calculated using the following relation [24]:

$$\lambda = \alpha \cdot C_p \cdot \rho \quad (1)$$

where α is the thermal diffusivity [mm^2/s], C_p is the specific heat capacity [$J/g \cdot K$] and ρ is the sample density [g/cm^3].

The thermal conductivity, heat capacity, thermal diffusivity, and density of the obtained samples were determined with an accuracy of ±3%, ±5%, ±3%, and ±0.01 g/cm^3, respectively. The accuracy of the activation energy estimation was of about ±5 kJ/mol.

The activation energy of the crystallization was estimated by measuring the kinetics of crystallization at heating rates of 5, 10, 20, and 40 °C/min, according to the methods of Kissinger [25] (2) and Ozava [26] (3).

$$\ln\left(\frac{T_x^2}{V}\right) = \frac{E}{R} \cdot \frac{1}{T_x} + C \quad (2)$$

$$\ln(V) = \frac{-E}{R} \cdot \frac{1}{T_x} + C \quad (3)$$

where V is the heating rate, R is the gas constant, E is the activation energy, and C is a fitting constant.

The pulverization of the metallic glass and the subsequent blending of the PET were carried out by the ball milling (BM) technique using a water-cooled high energy planetary ball mill (AGO-2S) with a rotation speed of 840 min^{-1}. Steel reactors and balls (4 mm diameter) were used. The mass ratio of the beads and the powder mixture was 10:1. The grinding time for pulverization of the glass ribbon was 45 min. The grinding time for mixing the metallic materials and the polymers was about 5 min.

The prepared composite powder mixture was placed into a cylindrical graphite die with 12.7 mm inside diameter, 30 mm outside diameter, and 30 mm height. The sample was also wrapped in a graphite sheet, 0.2 mm thick. The sintering was done using a spark plasma sintering system (SPS) (Labox 650, Sinter Land, Japan) [27–30] under the following conditions: heating rate 50 °C/min, maximum temperature of 245 °C, pressure up to 50 MPa, residence time 5 min. The parameters of the SPS configuration and the device schema are shown in Reference [27]. The SPS processing parameters, such as pressure, voltage, or pressing time, can be varied to achieve the required properties.

The schematic figure indicating all stages of the samples preparation is presented in the Figure 1.

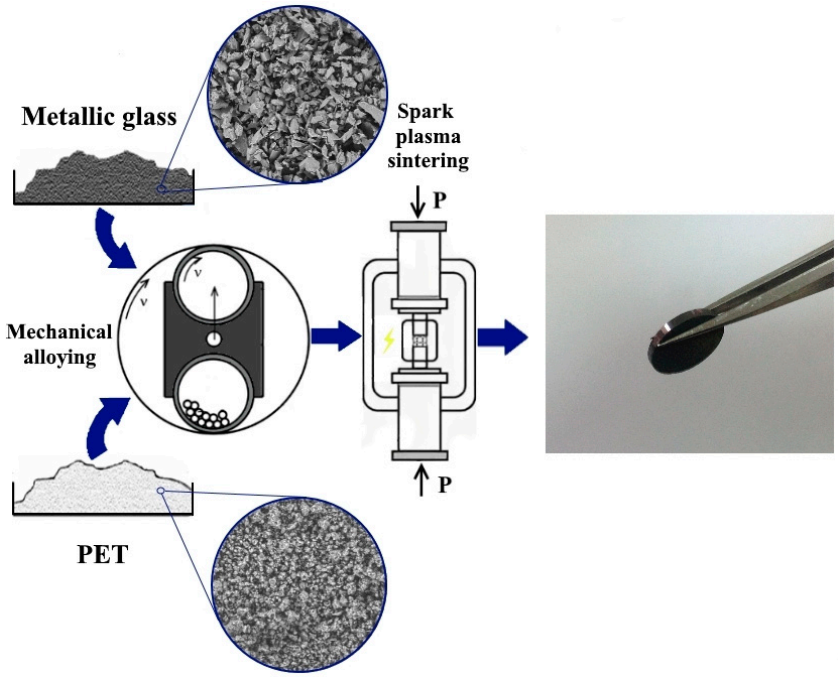

Figure 1. Scheme used for manufacturing samples using a ball milling technique and subsequent spark plasma sintering.

3. Results and Discussion

The XRD diffraction pattern of the $Al_{85}Y_8Ni_5Co_2$ bands contained only one amorphous halo (Figure 2a); no evidence of residual crystallinity peaks was detected. According to the XRD analysis, the curves are totally amorphous. DSC analysis of the ribbons showed that the metallic glass had a low transition temperature (T_g) of about 120 °C and a crystallization temperature (T_x) of about 260 °C (Figure 3a).

The main criterion for the selection of the polymeric material was its ability to get soft in the super cooled temperature region of the metallic glass phase. Polyethylene terephthalate (PET) is relative to this temperature range. This polymeric material is in the liquid state at a temperature close to the supercooled liquid region of the chosen metallic glass, and is capable of interacting with the metallic glass particles. Similarly, PET was chosen for its wide distribution and low cost.

The DSC curve of PET shows that, although the melting temperature of the polymer is 250 °C, it starts to change its properties and transform into a viscous liquid somewhat above 75 °C (Figure 2a). Thus, at temperatures above 250 °C both materials ($Al_{85}Y_8Ni_5Co_2$ metallic glass and PET) are in a viscous liquid state. Hence, it should be feasible to prepare the composite samples between their T_g and T_x.

To prepare bulk composite samples, starting with the SPS method, the initial materials must be in powder form. Therefore, grinding of the metallic glass ribbon ($Al_{85}Y_8Ni_5Co_2$) in a dispersed powder using the mechanical alloy method in a planetary ball mill was performed. It was found that the grinding process by ball milling results in the formation of the crystalline phases based on Al of approximately 20% (see Figure 2b and Table 1). For the SPS process, different temperatures from 200 °C and higher were applied, and the quality of the samples obtained was not so good. Hence, the temperature near T_g of the metallic glass $Al_{85}Y_8Ni_5Co_2$ (of approximately 250 °C) was chosen. However, the SPS process of the amorphous powder $Al_{85}Y_8Ni_5Co_2$ at 250 °C caused a small amount of crystalline phases to increase. In addition to the Al phase, the Al_9Co_2Ni phase was also found. Consequently, the total amount of the crystalline phases was about 25% (see Figure 2c and Table 1).

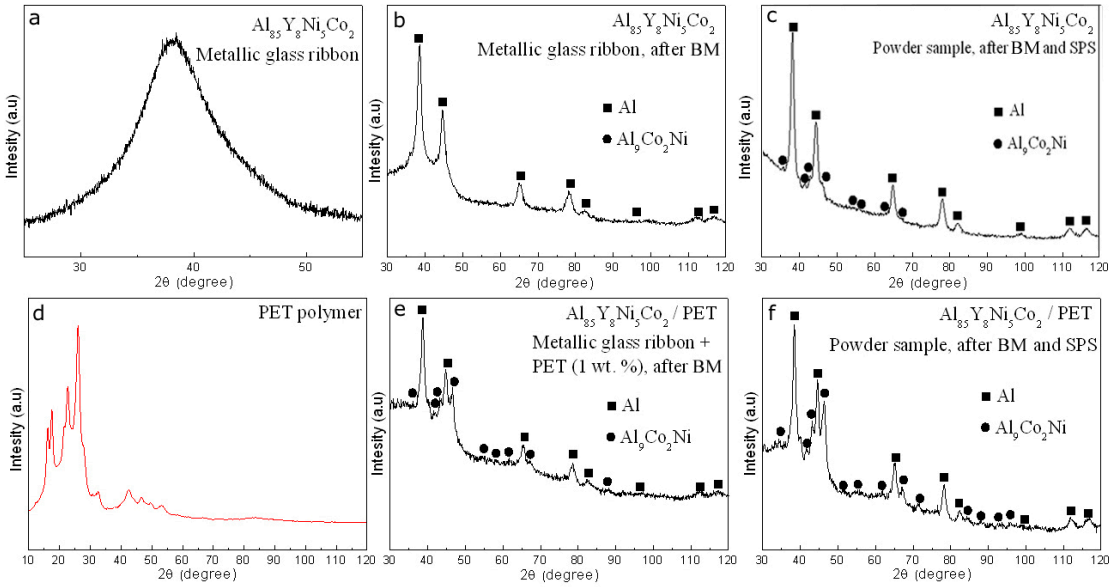

Figure 2. X-ray diffraction (XRD) pattern of the $Al_{85}Y_8Ni_5Co_2$ ribbon (**a**), $Al_{85}Y_8Ni_5Co_2$ ribbon, after ball milling (BM) (**b**), $Al_{85}Y_8Ni_5Co_2$ bulk sample, after BM and spark plasma sintering (SPS) (**c**) and polyethylene terephthalate (PET) powder (**d**), composite $Al_{85}Y_8Ni_5Co_2$/PET powder, obtained BM (**e**), composite $Al_{85}Y_8Ni_5Co_2$/PET bulk sample, obtained by BM and SPS (**f**).

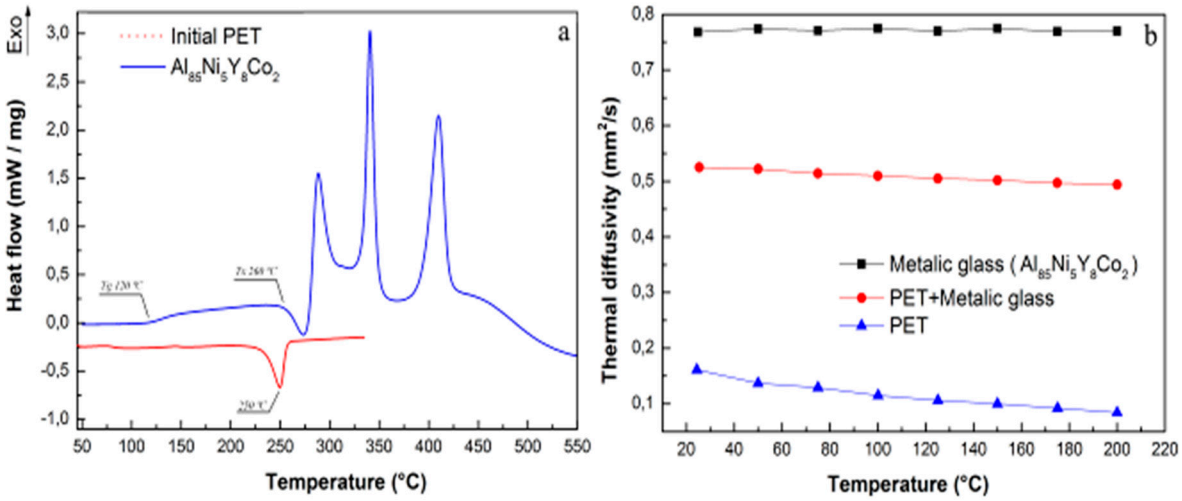

Figure 3. Differential scanning calorimetry (DSC) analysis of the $Al_{85}Y_8Ni_5Co_2$ ribbon sample and polyethylene terephthalate powder sample (**a**), and thermal conductivity of pure PET samples, $Al_{85}Y_8Ni_5Co_2$ metallic glass, and composite samples (**b**).

Table 1. Phase composition of the obtained samples.

Phase Composition	$Al_{85}Y_8Ni_5Co_2$, Ribbon	$Al_{85}Y_8Ni_5Co_2$, Ribbon, after BM	$Al_{85}Y_8Ni_5Co_2$ after BM and SPS	PET/Glass Composite Powder, after BM	PET/Glass Composite, after SPS
Amorphous	100%	80%	75%	70%	60%
Al (FCC)	-	20%	20%	20%	20%
Al_9Co_2Ni	-	-	5%	10%	20%

It should be recognized that the structure of the polymer after SPS is semi-crystalline/semi-amorphous, and that most of x-ray diffraction peaks are below 30 degrees 2θ (Figure 2d). To obtain

the composite samples, 1% by weight of PET polymer powders is added to $Al_{85}Y_8Ni_5Co_2$ powders during mechanical alloying. After ball milling, the amount of crystalline phase increases up to 30% (see Figure 2e and Table 1). After the SPS process at 250 °C of the composite powder ($Al_{85}Y_8Ni_5Co_2$/PET metal glass), the amount of crystalline phases increases to 40% (Figure 2f and Table 1).

The thermal conductivity analysis of the prepared bulk samples is presented in Table 2 and Figure 3b. It is clearly shown that the thermal conductivity of the composite material is reduced by adding only 1% by weight of PET, relative to the pure metal glass sample. The difference between the thermal conductivity of the composite sample and the metal glass sample is about 50%. This difference is much greater compared to the results presented in our previous works (in the case of composite materials with other polymers and metallic glass materials) [21,22]. It must also be taken into account that the bulk composite samples obtained by SPS were fragile. This reduction in thermal conductivity and brittleness of the bulk samples, obtained by the SPS, should be explained by the formation of the thin PET films on the boundaries between the metallic glass powder particles and, thus, the appearance of the photon scattering centers. In addition, this could be explained by the protective layer of Al oxide on the surface of the particles of metallic glass powder and the absence of diffusion reaction between the particles, as indicated in the previous work [21].

The SEM images of the bulk sample prepared by SPS are shown in Figure 4a. The compound after SPS is very porous. Some of the metallic glass particles are covered with the polymer (Figure 4b), and some of them were connected to each other by the necks (Figure 4c,d). However, such interactions between particles were not observed everywhere. The surface of the $Al_{85}Y_8Ni_5Co_2$ metallic glass strip and the surface of the overall sample of pure PET polymer, obtained by SPS, are shown in Figure 4e,f for comparison. The porous structure of the bulk samples was also responsible for the low thermal conductivity.

Table 2. Thermal properties and densities of the obtained samples.

Temperature Analysis, °C	**25**	**50**	**75**	**100**	**125**	**150**	**175**	**200**
$Al_{85}Y_8Ni_5Co_2$ metallic glass								
Thermal diffusivity, mm^2/s	0.768	0.774	0.771	0.775	0.770	0.775	0.769	0.770
Thermal conductivity, $W \cdot m^{-1} \cdot K^{-1}$	1.45	1.49	1.51	1.55	1.56	1.60	1.62	1.65
Heat capacity, J/(g·K)	0.584	0.595	0.606	0.617	0.628	0.640	0.651	0.662
Sample density, g/cm^3	3.235							
Polyethylene terephthalate (PET)								
Thermal diffusivity, mm^2/s	0.161	0.137	0.129	0.115	0.106	0.10	0.092	0.084
Thermal conductivity, $W \cdot m^{-1} \cdot K^{-1}$	0.220	0.255	0.274	0.266	0.249	0.246	0.241	0.239
Heat capacity, J/(g·K)	1.03	1.40	1.60	1.74	1.77	1.85	1.97	2.14
Sample density, g/cm^3	1.33							
Composite sample: $Al_{85}Y_8Ni_5Co_2$+ PET (1%)								
Thermal diffusivity, mm^2/s	0.525	0.522	0.514	0.51	0.505	0.502	0.497	0.494
Thermal conductivity, $W \cdot m^{-1} \cdot K^{-1}$	0.798	0.807	0.821	0.850	0.864	0.875	0.882	0.887
Heat capacity, J/(g·K)	0.59	0.60	0.62	0.647	0.664	0.677	0.689	0.697
Sample density, g/cm^3	2.577							

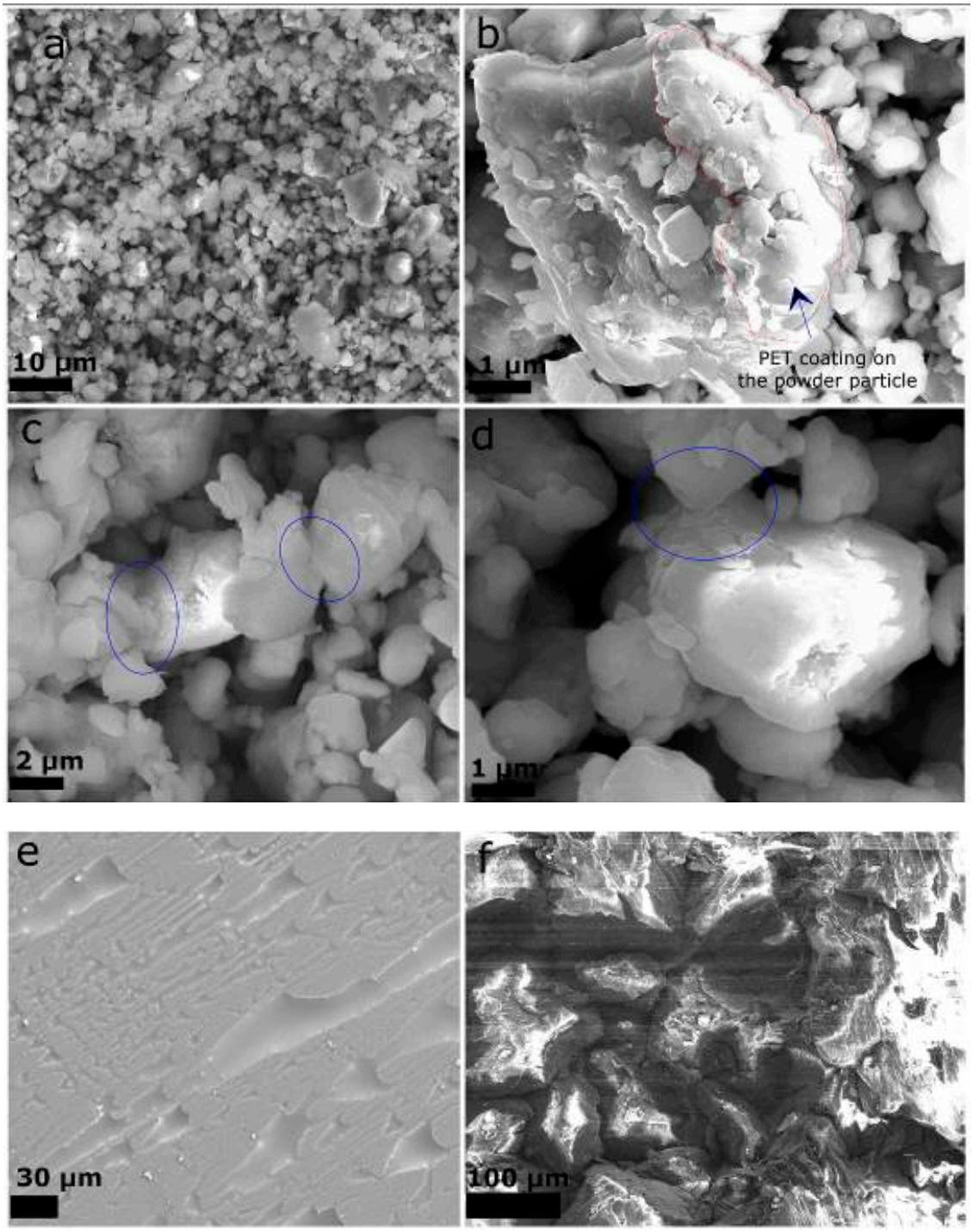

Figure 4. SEM images of the obtained samples: Surface of the composite sample $Al_{85}Y_8Ni_5Co_2$ + PET (1%) obtained by SPS (**a**), the particle coated by PET (**b**), neck formations between some of the particles during SPS process (**c**,**d**), surface of the $Al_{85}Y_8Ni_5Co_2$ ribbon sample (**e**), and polyethylene terephthalate bulk sample (**f**).

The activation energy of the crystallization process was calculated using the equations of Kissinger (2) and Ozava (3). These values are shown in Table 3 in comparison with the activation energies of other types of metallic glasses studied in our previous works ($Mg_{67.5}Ca_5Zn_{27.5}$ and $Cu_{54}Pd_{28}P_{18}$) [21,22]. The activation energy of the $Al_{85}Y_8Ni_5Co_2$ metallic glass is greater (Table 3); in addition, it is in a good correspondence with the activation energy of the metallic glasses based on Al, obtained in

Reference [31]. Therefore, we can assume that, indirectly, it influences the quality of the bulk composite samples. Therefore, at higher activation energies for crystallization, it is more difficult to initialize the interaction process between the metallic glassy particles and the mass transfer obtained between the two different materials in the neighboring particles.

Table 3. The activation energies of the crystallization process in the metallic glasses based on the $Al_{85}Y_8Ni_5Co_2$, $Mg_{67.5}Ca_5Zn_{27.5}$, and $Cu_{54}Pd_{28}P_{18}$ ribbons.

Metallic Glass Ribbon	$Al_{85}Y_8Ni_5Co_2$	$Mg_{67.5}Ca_5Zn_{27.5}$ [21]	$Cu_{54}Pd_{28}P_{18}$ [22]
	Activation Energy (E_{Tx}), kJ		
Calculated by Kissinger Equation (2)	303.5	140.9	302.7
Calculated by Ozava Equation (3)	313.5	147.1	311.8
Average value	309	144	307

4. Conclusions

A method was proposed that allows obtaining a composite material based on a polyethylene terephthalate and $Al_{85}Y_8Ni_5Co_2$ metallic glass. The method comprises SPS consolidation of the polymer blending with the metallic glass particles at a temperature near the temperature of the supercooled liquid of the metallic glass and the melting temperature of the PET.

The obtained composite samples have a superior thermal conductivity compared to the pure PET samples. The activation energy of the crystallization process has been calculated and compared with the activation energies of other types of metallic glasses used for composites preparation in previous works ($Mg_{67.5}Ca_5Zn_{27.5}$ and $Cu_{54}Pd_{28}P_{18}$). It was shown that the $Al_{85}Y_8Ni_5Co_2$ metallic glass has the highest activation energy in comparison with the other metallic glasses ($Mg_{67.5}Ca_5Zn_{27.5}$ and $Cu_{54}Pd_{28}P_{18}$). The relatively higher activation energy of the amorphous alloy studied in this research indicates its higher stability with respect to the crystallization process upon heating. However, significant oxidation of the surface of the alloy particles leads to a modification in the chemical composition of the surface layers of the material, and as a result, to a partial surface crystallization of the powder. This affects the quality of the composites produced, since the appearance of crystalline phases in metallic glass usually leads to deterioration of physical properties. The obtained results can be beneficial in terms of obtaining different antifriction composite materials based on metallic glass and self-lubricated polymers.

Author Contributions: V.Z., J.W. analyzed the data, wrote, reviewed, and edited of the manuscript; M.C., A.S., M.Z., A.S., D.M., E.S. performed the experiments; S.K. contributed materials and analysis tools; D.L., S.K. conceived and designed the experiments.

Funding: This research was funded by the Ministry of Education and Science of the Russian Federation, grant number: 11.1934.2017/ПЧ; by RFBR, grant number: 18-52-53027; by National Natural Science Foundation of China, grant number: 51811530101 and by the European Research Council under the ERC Advanced Grant INTELHYB, grant number: ERC-2013-ADG-340025.

Conflicts of Interest: The authors declare no conflict of interest.

References

1. Nicodemo, L.; Nicolais, L. Mechanical properties of metal/polymer composites. *J. Mater. Sci. Lett.* **1983**, *2*, 201–203. [CrossRef]
2. Inoue, A. Amorphous, nanoquasicrystalline and nanocrystalline alloys in Al-based systems. *Prog. Mater. Sci.* **1998**, *43*, 365–520. [CrossRef]
3. Jaschinski, W.; Wolf, W.; König, U.; Hartwig, J. Amorphe Metalle-Entwicklung einer neuen Werkstoffklasse. *Techn. Mitt. Krupp-Forsch.-Ber.* **1981**, *39*, 1–12.

4. Hillenbrand, H.G. Die Festigkeit metallischer Gläser auf der Grundlage von Eisen-Bor im schnell abgekühltem und angelassenem. *Zustand. VDI-Zeitschrift* **1983**, *125*, 409–410.
5. Sanchez, C.; Julián, B.; Belleville, P.; Popall, M. Applications of hybrid organic–inorganic nanocomposites. *J. Mater. Chem.* **2005**, *15*, 3559–3592. [CrossRef]
6. Briscoef, B.; Kremnitzer, S. A study of the friction and adhesion of polyethyleneterephthalatemonofilaments. *J. Phys. D Appl. Phys.* **1979**, *12*, 505–516. [CrossRef]
7. Yusof, F.; Miyashita, Y.; Seo, N.; Mutoh, Y.; Moshwan, R. Utilising friction spot joining for dissimilar joint between aluminium alloy (A5052) and polyethylene terephthalate. *Sci. Technol. Weld. Join.* **2012**, *17*, 544–549. [CrossRef]
8. Kundig, A.; Schweizer, T.; Schafler, E.; Loffler, F. Metallic glass/polymer composites by co-processing at similar viscosities. *Scripta Mater.* **2007**, *56*, 289–292. [CrossRef]
9. Li, S.; Louzguine-Luzgin, D.V.; Xie, G.; Sato, M.; Inoue, A. Development of novel metallic glass/polymer composite materials by microwave heating in a separated H-field. *Mater. Lett.* **2010**, *64*, 235–238. [CrossRef]
10. Zhang, B.; Zhao, D.; Pan, M.; Wang, W.; Greer, A. Amorphous metallic plastic. *Phys. Rev. Lett.* **2005**, *94*, 205502. [CrossRef]
11. Schroers, J.; Lohwongwatana, B.; Johnson, W.L.; Peker, A. Gold based bulk metallic glass. *Appl. Phys. Lett.* **2005**, *87*, 061912. [CrossRef]
12. Torrisi, V.; Ruffino, F. Metal-Polymer Nanocomposites: (Co-) Evaporation/(Co) Sputtering Approaches and Electrical Properties. *Coatings* **2015**, *5*, 378–424. [CrossRef]
13. Grubbs, R. Hybrid metal-polymer composites from functional block copolymers. *J. Polym. Sci. Part A Polym. Chem.* **2005**, *43*, 4323–4336. [CrossRef]
14. Wang, Z.; Scudino, S.; Stoica, M.; Zhang, W.; Eckert, J. Al-based matrix composites reinforced with short Fe-based metallic glassy fiber. *J. Alloy. Compd.* **2015**, *651*, 170–175. [CrossRef]
15. Wang, Z.; Prashanth, K.; Scudino, S.; Chaubey, A.; Sordelet, D.; Zhang, W.; Li, Y.; Eckert, J. Tensile properties of Al matrix composites reinforced with in-situ devitrified $Al_{84}Gd_6Ni_7Co_3$ glassy particles. *J. Alloy. Compd.* **2014**, *586*, S419–S422. [CrossRef]
16. Zhang, W.; Hu, Y.; Wang, Z. Formation of Nanoscale Metallic Glassy Particle Reinforced Al-Based Composite Powders by High-Energy Milling. *Metals* **2017**, *7*, 425. [CrossRef]
17. Wang, Z.; Qu, R.; Scudino, S.; Sun, B.; Konda, P.; Louzguine-Luzgin, D.; Chen, M.; Zhang, Z.; Eckert, J. Hybrid Nanostructured Aluminum Alloy with Super-High Strength. *NPG Asia Mater.* **2015**, *7*, 229. [CrossRef]
18. Wang, Z.; Georgarakis, K.; Nakayama, K.; Li, Y.; Xi, G.; Louzguine-Luzgin, D.; Yavari, A. Microstructure and mechanical behavior of metallic glass fiber-reinforced Al alloy matrix composites. *Sci. Rep.* **2016**, *6*, 24384. [CrossRef]
19. Beygelzimer, Y.; Kulagin, R.; Estrin, Y.; Toth, L.; Kim, H.; Latypov, M. Twist Extrusion as a Potent Tool for Obtaining Advanced Engineering. *Mater. A Rev. Adv. Eng. Mater.* **2017**, *19*, 1600873. [CrossRef]
20. Sanchez, C.; Soler-Illia, A.; Ribot, F.; Lalot, T.; Mayer, C.; Cabuil, V. Designed Hybrid Organic-Inorganic Nanocomposites from Functional Nanobuilding Blocks. *Chem. Mater.* **2001**, *13*, 3061–3083. [CrossRef]
21. Zadorozhnyy, M.Yu.; Chukov, D.I.; Churyukanova, M.N.; Gorshenkov, M.V.; Zadorozhnyy, V.Yu.; Stepashkin, A.A.; Tsarkov, A.A.; Louzguine-Luzgin, D.V.; Kaloshkin, S.D. Investigation of contact surfaces between polymer matrix and metallic glasses in composite materials based on high-density polyethylene. *Mater. Des.* **2016**, *92*, 306–312. [CrossRef]
22. Zadorozhnyy, V.Yu.; Gorshenkov, M.V.; Churyukanova, M.N.; Zadorozhnyy, M.Yu.; Stepashkin, A.A.; Moskovskikh, D.O.; Ketov, S.V.; Zinnurova, L.Kh.; Sharma, A.; Louzguine-Luzgin, D.V.; et al. Investigation of structure and thermal properties in composite materials based on metallic glasses with small addition of polytetrafluoroethylene. *J. Alloy. Compd.* **2017**, *707*, 264–268. [CrossRef]
23. Shelekhov, E.V.; Sviridova, T.A. Modeling of the motion and heating of balls in a planetary ball mill: Effect of processing conditions on the mechanical activation products of Ni-Nb powder mixtures. *Materialovedenie* **1999**, *10*, 13–22.
24. Olifirov, L.K.; Kaloshkin, S.D.; Zhang, D. Study of thermal conductivity and stress-strain compression behavior of epoxy composites highly filled with Al and Al/f-MWCNT obtained by high-energy ball milling. *Compos. Part A* **2017**, *101*, 344–352. [CrossRef]
25. Ozava, T. Kinetic analysis of derivative curves in thermal analysis. *J. Therm. Anal.* **1970**, *2*, 301–324.
26. Kissinger, H.E. Reaction Kinetics in Differential Thermal Analysis. *Anal. Chem.* **1957**, *29*, 1702. [CrossRef]

27. Orru, R.; Licheri, R.; Locci, A.; Cincotti, A.; Cao, G. Consolidation/synthesis of materials by electric current activated/assisted sintering. *Mater. Sci. Eng. R.* **2009**, *63*, 127–287. [CrossRef]
28. Moskovskikh, D.; Lin, Y.; Rogachev, A.; Mcginn, P.; Mukasyan, A. Spark plasma sintering of SiC powders produced by different combustion synthesis routes. *J. Eur. Ceram. Soc.* **2015**, *35*, 477–486. [CrossRef]
29. Abedi, M.; Moskovskikh, D.O.; Rogachev, A.S.; Mukasyan, A.S. Spark Plasma Sintering of Titanium Spherical Particles. *Metall. Mater. Trans. B* **2016**, *47*, 2725–2731. [CrossRef]
30. Moskovskikh, D.O.; Song, Y.; Rouvimov, S.; Rogachev, A.S.; Mukasyan, A.S. Silicon carbide ceramics: Mechanical activation, combustion and spark plasma sintering. *Ceram. Int.* **2016**, *42*, 12686–12693. [CrossRef]
31. Louzguine, D.V.; Inoue, A. Crystallization behaviour of Al-based metallic glasses below and above the glass-transition temperature. *J. Non-Cryst. Solids* **2002**, *311*, 281–293. [CrossRef]